Peer-reviewed version available at Metals 2020, 10, 1084; doi:10.3390/met10081084

Type of the Paper (Article)

Modelling of Fluid Flow and Residence Time Distribution in a Five-strand Tundish

Dong-Yuan Sheng [1,2,*] **Qiang Yue** [3]

[1]Department of Materials Science and Engineering, Royal Institute of Technology, 10044, Stockholm, Sweden; Email: shengdy@kth.se
[2]Westinghouse Electric Sweden AB, 72163, Västerås, Sweden
[3]School of Metallurgical Engineering, Anhui University of Technology, Ma'anshan 243002, China; Email: yueqneu@163.com
*Correspondence: shengdy@kth.se, +46 8 790 84 67

Abstract: The quantified residence time distribution (RTD) provides a numerical characterization of mixing in the continue casting tundish, thus allowing the engineer to better understand the metallurgical performance of the reactor. This paper describes a computational fluid dynamic (CFD) modelling study for analyzing the flow pattern and the residence time distribution in a five-strand tundish. Two passive scalar transport equations are applied to separately calculate the E-curve and F-curve in the tundish. The numerical modelling results are compared to the water modelling results for the validation of the mathematical model. The volume fraction of different flow regions (plug, mixed and dead) and the intermixing time during the ladle changeover are calculated to study the effects of the flow control device (FCD) on the tundish performance. The result shows that a combination of the U-baffle with deflector holes and the turbulence inhibitor has three major effects on the flow characteristics in the tundish: i) reduce the extent of the dead volume; ii) evenly distribute the liquid streams to each strand and iii) shorten the intermixing time during the ladle changeover operation.

Keywords: mathematical model, water model, tundish, residence time distribution, mixing

1 Introduction

The tundish, working as a buffer and distributor of liquid steel between the ladle and continuous casting molds, plays a key role in affecting the performance of casting and solidification, as well as the quality of final products, referred to as "Tundish Metallurgy". With the continuing emphasis on the superior steel quality, a modern steelmaking tundish is designed to provide maximum opportunity for the control of molten steel flow, heat transfer, mixing and inclusion removal. Considerable research efforts have been made in academia and industry over many decades to fully exploit and enhance the metallurgical performance of the tundish [1-4].

In metallurgical engineering, the residence time distribution (RTD) of the fluid is used as an index of the performance of the reactors. The RTD characteristics of a given tundish can be studied through the pulse injection of inert tracer at the inlet in the water model experiment and monitored by the change of tracer concentration at the outlet. The RTD analysis e.g. the mean residence time, the plug flow volume, the dead volume and the mixed volume are used to estimate the tundish performance. The dye tracer visualizes the flow pattern, which may put the results obtained by the RTD analysis in proper perspective. These experimental studies provide useful input data to validate the developed mathematical model.

Peer-reviewed version available at Metals 2020, 10, 1084; doi:10.3390/met10081084

Two categories of RTD have been extensively investigated in the tundish: i) E-curve, an instantaneous addition of tracer at inlet, which is used to describe the fluid flow, and further to optimize the FCD designs such as weirs, dams, turbulence inhibitor and baffles; ii) F-curve, a continuous addition of tracers, which is used to describe the chemical composition mixing during the ladle changeover operations.

A large number of mathematical modelling studies have been carried out to analyze the flow and the RTD in the tundish, including: i) the study of FCD configurations; ii) the study of external stirring (e.g. gas-stirring and electromagnetic stirring); iii) the study of simulation model (e.g. fluid flow, turbulence, particle dispersion, isothermal/thermal, steady/transient). Table 1 lists the published modelling studies with the consideration of the flow control devices and RTD analysis in the tundish [5-20]. It shows that Computational Fluid Dynamics (CFD) has become a useful and promising tool that can potentially predict accurately of the mixing in the tundish.

This study focuses on the determination of the characteristics of RTD in a five-strand tundish. In the following paper, the description of the CFD model and the theoretical basis of RTD analysis are given. Sensitivity studies of the mesh size have been conducted for the verification of the mathematical modelling. A 1:3 scale water model is used to measure the tracer concentration for the RTD curves. The simulated results are in contrast with the measured results to validate the developed mathematical model. The analysis results of the fluid flow, the RTD E-curve and F-curve of the different designs are presented with the aim of achieving optimum control of the molten steel flow in the tundish.

2 Methods

2.1 Model Description

The CFD software STAR-CCM+ v.13 is utilized to simulate the fluid flow and the tracer dispersion. The assumptions made for the mathematical model are described below:

- The model is based on a 3-D standard set of the Navier-Stokes equations. The continuous phase is treated by a Eulerian framework (using averaged equations).
- Two additional passive scalar transport equations are solved to separately describe the E-curve and the F-curve.
- The liquid flow has been assumed to be isothermal and in steady state.
- The realizable k-ε model has been used to describe the turbulence.
- The free surface is flat and kept at a fixed level. The slag layer is not included in the tundish.

In the mathematical model, the conservation of a general flow variable ϕ, for example the density, momentum, within a finite control volume can be expressed as a balance between the various processes. The calculation of single-phase incompressible flow is accomplished by solving the mass and momentum conservation equations. The equations solved in CFD code are written in a general form as:

$$\rho \frac{\partial \bar{\phi}}{\partial t} + \rho \bar{u_j} \frac{\partial \bar{\phi}}{\partial x_j} - \frac{\partial}{\partial x_j}\left[\Gamma_{\phi,eff} \frac{\partial \bar{\phi}}{\partial x_j}\right] = S_{\phi} \quad (1)$$

Peer-reviewed version available at Metals 2020, 10, 1084; doi:10.3390/met10081084

Table 1. Summary of mathematical modelling investigations on residence time distribution (RTD) in the tundish

Reference	Model[1]	Code	Design				Numerical Model				Parameter Study [2]
			Strand	Fluid[3]	FCD[4]	Gas	Fluid [5]	Turb.[6]	Inclu.[7]	RTD[8]	
S. López-Ramirez(1998) [5]	N	-	2	S	B, TI	-	-	k-ε	-	E	SFR, FCD, TC
Vargas-Zamora (2004) [6]	N, P	-	1	W	TI, D	-	-	-	-	F	GFR
Zhong (2008) [7]	P	-	2	W	TI, D, W	N_2	-	-	-	E	TC, FCD, GFR
Bensouici (2009) [8]	N, P	Fluent	1	W	W, D	-	-	k-ε	-	E	MS, FCD
Zheng (2011) [9]	N, P	CFX	2	S	TI, B	Ar	Eu	k-ε	La	E	TC, GFR, IS
Chen(2013) [10]	N, P	FLUENT	1	S, W	W	Ar	Eu	k-ε	La	E	TC, FCD, IS
Chen (2015) [11]	N, P	PHOENICS	1	W	SR, D, W, TI	-	-	k-ε	-	E	MS, TS, TP
Chang (2015) [12]	N, P	FLUENT	7	S, W	TI, B	Ar	Eu	k-ε	La	E	GFR, FCD
Devi (2015) [13]	N, P	FLUENT	2	S, W	D	Ar	Eu	k-ε	-	E	FCD, GFR
He (2016)[14]	N, P	FLUENT	5	S, W	TI, B	-			-	E	TC, SFR
Neves (2017) [15]	N, P	CFX	2	W	SR, D, W	Air	Eu	k-ε	-	E	GFR, FCD
Wang(2017) [16]	N, P	FLUENT	8	S	TI,	-	-	k-ε	La	E	TC, FCD, IS
Aguilar-Rodriguez(2018)[17]	N	FLUENT	1	S	-	Ar	VOF	k-ε	La	E	GFR, TC, FCD
Yang (2019) [18]	N	CFX	2	S	D, TI	-	-	k-ε	La	E	FCD, TC
Wang (2020) [19]	N	FLUENT	2	S	W, TI, F	-	Eu	k-ε	La	E	IS, FCD, TC

[1]N: numerical model; P: physical model
[2] SFR: steel flow rate; GFR: gas flow rate; TC: tundish configuration; MS: mesh size; TS: time step; TM: turbulence model; ID: inlet depth; IS: inclusion size; FCD: Flow control devices;
[3] W: water; S: steel
[4] FCD: flow control devices; SR: stop rod; D: dam; W; weir; TI: Turbulence inhibitor: F: filter; B: baffles
[5] Eu: eulerian; VOF: volume of fluid;
[6]Turb.: turbulence
[7]Inclu.: inclusion; La: lagrangian;
[8]E:E-curve; F:F-curve

Preprints (www.preprints.org) | NOT PEER-REVIEWED | Posted: 16 July 2020 doi:10.20944/preprints202007.0354.v1

Peer-reviewed version available at Metals 2020, 10, 1084; doi:10.3390/met10081084

Where ϕ represents the solved variable, $\Gamma_{\phi,eff}$ is the effective diffusion coefficient, S_ϕ is the source term, x_j are the Cartesian coordinates, u_j are the corresponding average velocity components, t is the time and ρ is the density. The first term expresses the rate of change of ϕ with respect to time, the second term expresses the convection (transport due to fluid- flow), the third term expresses the diffusion (transport due to the variation of ϕ from point to point) where $\Gamma\phi$ is the exchange coefficient of the entity ϕ in the phase and the fourth term expresses the source terms (associated with the creation or destruction of variable ϕ).

2.2 Fluid Flow

The Eulerian approach with the realizable *k-ε* turbulence model are applied to calculate the single-phase phenomenon in the tundish. The liquid steel flow is defined as a three-dimensional flow with the constant density. Equation 2 and 3 are the governing equations used to describe the continuous phase.

Continuity: $$\frac{\partial(\rho u_j)}{\partial x_j} = 0 \quad (2)$$

Momentum: $$\rho u_j \frac{\partial u_i}{\partial x_j} = -\frac{\partial P}{\partial x_i} + \frac{\partial}{\partial x_j}\left[(\mu + \mu_t)\left\{\frac{\partial u_i}{\partial x_j} + \frac{\partial u_j}{\partial x_i}\right\}\right] + \rho g_i + S_F \quad (3)$$

Realizable *k-ε* model:

$$\frac{\partial}{\partial t}(\rho k) + \frac{\partial}{\partial x_j}(\rho k u_j) = \frac{\partial}{\partial x_j}\left[\left(\mu + \frac{\mu_t}{\sigma_k}\right)\frac{\partial k}{\partial x_j}\right] + G_k + G_b - \rho\varepsilon - Y_M + S_k \quad (4)$$

$$\frac{\partial}{\partial t}(\rho \varepsilon) + \frac{\partial}{\partial x_j}(\rho \varepsilon u_j) = \frac{\partial}{\partial x_j}\left[\left(\mu + \frac{\mu_t}{\sigma_\varepsilon}\right)\frac{\partial \varepsilon}{\partial x_j}\right] + \rho C_1 S\varepsilon - \rho C_2 \frac{\varepsilon^2}{k + \sqrt{\nu\varepsilon}} + C_{1\varepsilon}\frac{\varepsilon}{k} C_3 G_b + S_\varepsilon \quad (5)$$

Where k is the turbulent kinetic energy; ε is the turbulent energy dissipation rate; μ is the molecular viscosity; μ_t is the turbulent viscosity; G_k represents the generation of turbulent kinetic energy due to the mean velocity; Y_M represents the contribution of the fluctuating dilatation in compressible turbulence to the overall dissipation rate; υ is the kinematic viscosity; σ_k and σ_ε are the turbulent Prandtl numbers for k and ε respectively.

The success of numerical prediction methods depends to a great extent on the performance of the turbulence model used. The realizable *k-ε* model is substantially better than the standard *k-ε* model for many applications and can generally be relied upon to give answers that are at least as accurate. The realizable *k-ε* model has been implemented in STAR-CCM+ with a two-layer approach, which enables it to be used with fine meshes that resolve the viscous sublayer [20].

2.3 Tracer Dispersion

Tracer dispersion experiments are conducted to understand the flow pattern in the five-strand tundish. To calculate the concentration of the additive tracer, the transport of two passive scalars (E-curve and F-curve) are simulated in a Eulerian framework by solving a filtered advection-diffusion equation. The passive scalar transport equations are solved at each time step once the fluid filed is calculated and reads.

$$\rho \frac{\partial \bar{c}}{\partial t} + \rho \bar{u}_j \frac{\partial \bar{c}}{\partial x_j} - \frac{\partial}{\partial x_j}\left[D_{eff}\frac{\partial \bar{c}}{\partial x_j}\right] = 0 \quad (6)$$

Where, the effective diffusivity, D_{eff}, is the sum of the molecular and turbulent diffusivity. The velocity field is solved from a steady-state simulation and remained constant during the calculation of the two passive scalars.

Preprints (www.preprints.org) | NOT PEER-REVIEWED | Posted: 16 July 2020 doi:10.20944/preprints202007.0354.v1

Peer-reviewed version available at Metals 2020, 10, 1084; doi:10.3390/met10081084

The RTD is a statistical representation of the time spent by an arbitrary volume of the fluid in the tundish. The RTD curve is used to analyze the different effective flow volumes, such as the plug volume, the dead volume and the mixed volume. As shown in Figure 1, E(t)dt is the probability that a fluid element enters the vessel at *t*=0 and exits between time t and t+dt.

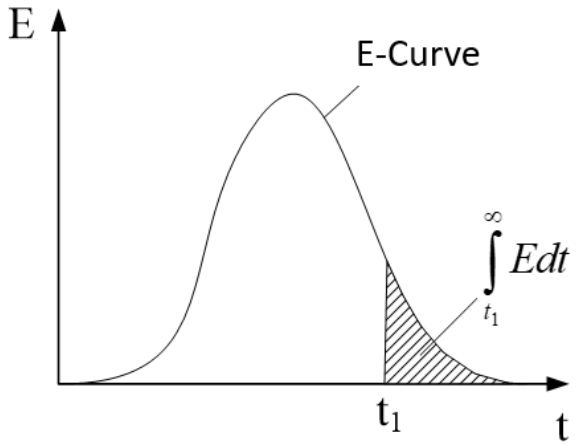

Figure 1 Residence time distribution (RTD) function

The simplest and most direct way of finding the E-curve uses a nonreactive tracer. E-curve can be plotted based on the dimensionless outlet concentration (C-curve) measured in the water model experiment. Actual mean residence time is presented in Equation 7.

$$\bar{\tau} = \int_0^{\infty} tC(t)dt \tag{7}$$

Theoretical residence time (τ) is given by

$$\tau = V_t/Q \tag{8}$$

Where Vt is the volume of tundish and Q is the volumetric flow rate.

The dimensionless outlet concentration (Ci) and time (θ) are given by

$$C_i = C/C_0, \theta = t/\bar{\tau} \tag{9}$$

$$d\theta = dt/\bar{\tau}, \ \bar{\theta} = \bar{\tau}/\bar{\tau} = 1 \tag{10}$$

Where C_0 is the concentration that corresponds to the condition where the added tracer is uniformly distributed in the tundish.

The existence of a dead volume can significantly decrease the active volume of tundish and reduce the residence times of liquid in the vessel. The increase in the dead volume fraction proves to be detrimental for the mixing.

In the tundish, the plug flow volume (V_p), the mixed flow volume (V_m) and the dead volume (V_d) have been calculated through Equation 11-13.

Fraction of dead volume, $V_d = 1 - \frac{\bar{\tau}}{\tau}$ (11)

Fraction of plug volume, $V_P = (\theta_{min} + \theta_{peak})/2$ (12)

Fraction of plug volume, $V_m = 1 - V_d - V_m$ (13)

Where, θ_{min} is the minimal dimensionless time at the tundish outlet and θ_{peak} is the peak dimensionless time at the tundish outlet.

Another common RTD expression is the cumulative distribution function F(t), i.e. the F-curve. F-curve is a fraction of the liquid that has a residence time less than time (t) and can be obtained by making a continuous addition of tracers at inlet. The concentration of tracer in the outlet stream is the F-curve. The relation between F(t) and E(t) is as follows:

$$F(t) = \int_0^t E(t)dt \quad (14)$$

Because F-curve has the integral property, it cannot reflect the transient or local information with the same resolution as E-curve. In this study, two passive scalar equations are solved in the CFD model: (i) an instantaneous addition of tracer at inlet (E-curve); (ii) a continuous addition of tracers at inlet (F-curve).

2.4 Modelling Descriptions

2.4.1 Water model

The geometrical dimensions of an in-plant 35-tonne tundish are illustrated in Figure 2. Steel flow rate is between 1.4 and 2.2 tonnes/min. Four cases with different tundish configurations are selected and comparatively studied. They are:

- Case 1- bare tundish;
- Case 2- tundish with turbulence inhibitor
- Case 3- tundish with U-baffle (with deflector holes)
- Case 4- tundish with U-baffle (with deflector holes) and turbulence inhibitor.

Peer-reviewed version available at Metals 2020, 10, 1084; doi:10.3390/met10081084

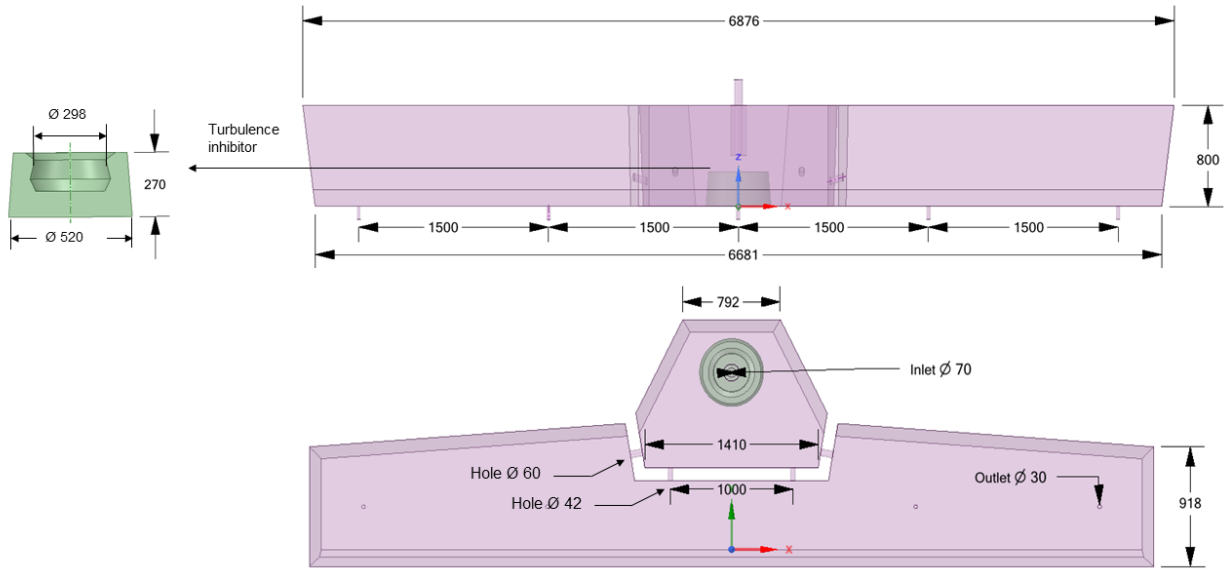

Figure 2 Dimensions of 5-strand tundish and turbulence inhibitor (unit: mm)

The parameters used in the water model are calculated by Froude similarity criterion, according to the expression below.

Geometrical similarity: $l_m/l_p=\lambda$ (15)

Froude similarity: $Fr=u^2/gl$ (16)

The scaled down velocity and water flow rate are correlated according to

$u_m/u_p=\lambda^{1/2}$ (17)

$Q_m/Q_p=\lambda^{5/2}$ (18)

Where, Fr is the Froude number; u is the velocity($m\cdot s^{-1}$); g is the acceleration of gravity ($m\cdot s^{-2}$); l is the length (m); Q is the volumetric flow rate ($m^3\cdot s^{-1}$) and λ *is the* length scale (1/3 in this study). The subscript m and p represent model and prototype, respectively.

Preprints (www.preprints.org) | NOT PEER-REVIEWED | Posted: 16 July 2020 doi:10.20944/preprints202007.0354.v1

Peer-reviewed version available at Metals 2020, 10, 1084; doi:10.3390/met10081084

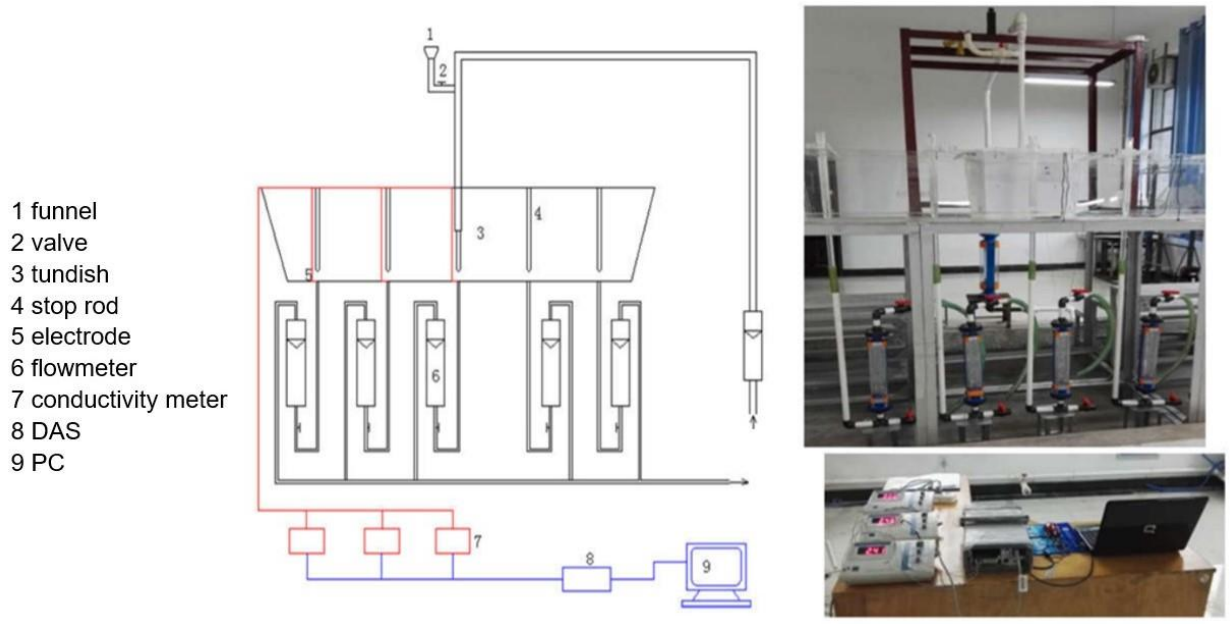

Figure 3 Schematic diagram and plexiglass model for water model of tundish

A 1:3 scale water model of the industrial prototype is used for the experimental analysis. The water model is made of plexiglass. The water model experiment is carried out considering the dispersion of tracer concentration in order to work out the characteristics of RTD curves. Water solution of NaCl is used as a tracer. The pulse stimulus-response technique is used to measure and obtain the RTD E-curves. When the assumed liquid level in the water model is reached and the flow is stabilized, a certain amount of saturated NaCl solution is quickly poured into the inlet as a tracer. The change of tracer concentration is registered continuously at the outlets from water model. The time and concentration are transformed to the dimensionless value in order to compare the obtained flow characteristics.

2.4.2 CFD geometry and mesh

To create the geometry for CFD calculation, the first step is to build up a 3D-CAD model by using the Ansys Spaceclaim V19.1. Half of the water model of the five-strand tundish is taken as the computational domain considering the symmetry of the tundish, illusrated in Figure 4. The volume mesh is generated in Star-CCM+ V13.04, utilizing the trimmer and prism layer meshing options. Three prism layers are generated next to all the walls. The surface mesh is generated first. Then the volume mesh is built based on the surface mesh by adjusting the growth rate and the biggest mesh size. A base mesh size of 0.003m is used in this study. The input parameters for the simulation are listed in Table 2. The surface average y+ value in the first layer of the mesh near the wall is 1.5. The final CFD model owns a trimmer mesh of 2 million cells in the computing domain.

Preprints (www.preprints.org) | NOT PEER-REVIEWED | Posted: 16 July 2020 doi:10.20944/preprints202007.0354.v1

Peer-reviewed version available at Metals 2020, 10, 1084; doi:10.3390/met10081084

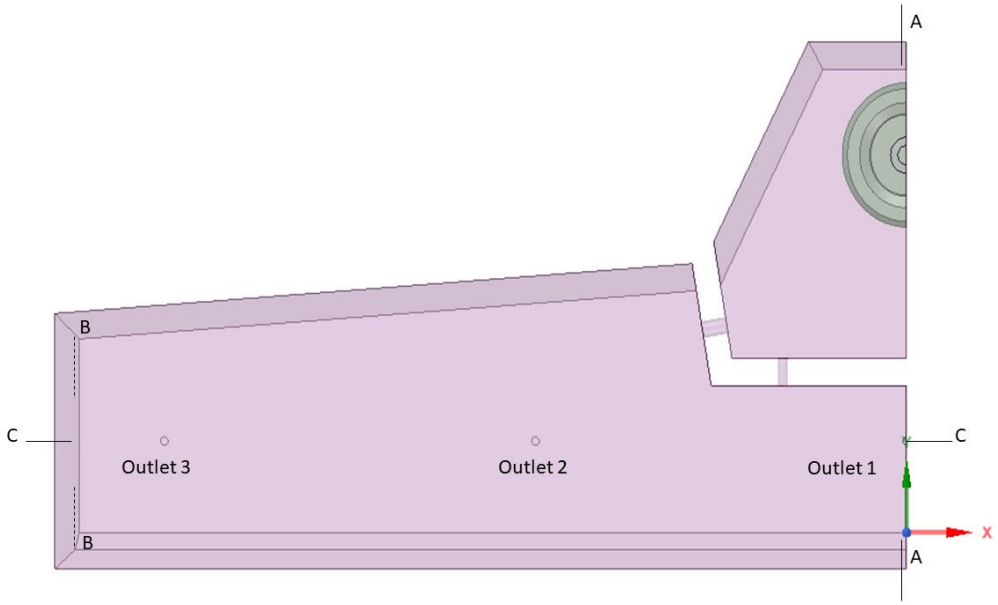

Figure 4 Computational domain in numerical modelling (one-half of the 5-strand tundish)

2.4.3 Initial and Boundary conditions

Liquid phase

The density and viscosity of water in numerical modelling are set to be 998 kg·m^{-3} and 8.9×10^{-4} Pa·s. No-slip conditions are applied at all solid surfaces for the liquid phase. A constant inlet velocity is used. At the tundish outlet, the outflow boundary condition is applied. A wall function is applied to bridge the viscous sub-layer and provide the near-wall boundary conditions for the average flow and the turbulence transport equations. The wall conditions are connected by means of empirical formulae to the first grid node close to the solid surfaces.

Tracer

Zero mass transfer flux is set at all walls and free surface for the passive scalar equation solutions. To solve the passive scalar equation (1) for E-curve, at t=0~2 s the mass fraction of tracer at the inlet is set to be equal to 1. When t>2s it is given as zero. To solve the passive scalar equation (2) for F-curve, the mass fraction of the tracer at inlet is set to be equal to 1 for all the time steps. The concentration of the tracer at the outlet has been monitored from t=0 and the RTD curves are obtained from the numerical calculation.

2.4.4 Solution procedure

The simulations are started by solving the steady state flow and the turbulence equations until a converged flow field is obtained. Then, the flow and turbulence equations are turned off. The passive scalar equations and the transient solver are activated. At this stage the mass fraction of the tracer at the inlet boundary is defined by the user field functions.

The discretized equations are solved in a segregated manner with the semi-implicit method for the pressure-linked equations (SIMPLE) algorithm. The second-order upwind scheme is used to calculate the

Preprints (www.preprints.org) | NOT PEER-REVIEWED | Posted: 16 July 2020 doi:10.20944/preprints202007.0354.v1

Peer-reviewed version available at Metals 2020, 10, 1084; doi:10.3390/met10081084

convective flux in the momentum equations. The solution is judged to be converged when the residuals of all flow variables are less than 10^{-4}, together with the stability of the velocity and the turbulence at the key monitor points. The under-relaxation parameter of flow calculations for the pressure, the velocity and the turbulence is 0.2, 0.8 and 0.8, respectively.

Utilization of an adequately refined and high-quality mesh is an important step in achieving accuracy in numerical simulations. As shown in Figure 5, a mesh independency study has been carried out to estimate an appropriate mesh density for the RTD analysis. Table 2 displays the calculated RTD parameters and volume fraction of flow with different mesh sizes. Comparing the results of three mesh sizes, the difference of volume fraction of the plug flow, mixed flow and dead flow are less than 2%, 3% and 1%, respectively. An acceptable mesh independent solution is obtained based on the observations above. With the considerations of the computing load and the near wall resolution, the computations are carried out with 2 million cells (Mesh 2) and the reference mesh size is 0.003 m.

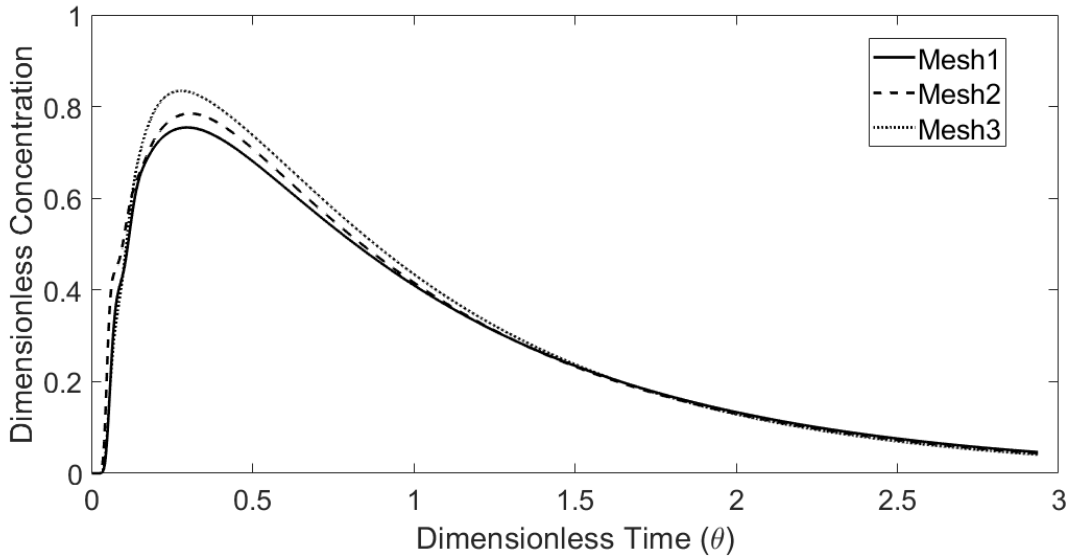

Figure 5 Comparison of calculated E-curves with different CFD mesh number (Data is available in the Supplementary Material)

Table 2 calculated RTD parameters and volume fraction of flow with different mesh size

Mesh	Mesh Number	Mesh size(m)	t_{theo}(s)[1]	t_{min}(s)	t_{max}(s)	t_{mean}(s)	V_p(%)	V_m(%)	V_d(%)
1	4 Million	0.002	749	31	222	685	17	75	9
2	2 Million	0.003	749	26	229	669	17	72	11
3	1 Million	0.004	749	30	208	664	16	73	11

[1] t_{theo}: theoretical residence time; t_{min}: minimum breakthrough time; t_{max}: time corresponding to peak concentration; t_{mean}: mean residence time. V_p: plug flow. V_d: dead volume; V_m: mixed flow

3 Results and Discussions

3.1 Flow Pattern

Preprints (www.preprints.org) | NOT PEER-REVIEWED | Posted: 16 July 2020 doi:10.20944/preprints202007.0354.v1

Peer-reviewed version available at Metals 2020, 10, 1084; doi:10.3390/met10081084

The flow patterns of the four studied cases are observed and compared thorough the following view planes, as illustrated in Figure 4:

- View A: Longitudinal plane of inlet
- View B: Horizontal plane (close to bottom)
- View C: Longitudinal plane of all the outlets

The entering flow with high momentum hits the bottom of the tundish, moves along the sidewall of the pouring chamber and then drives back to the incoming jet, forming a clockwise recirculation nearby the inlet region (Figure 6a and 6c). When the tundish is equipped with turbulence inhibitor, the entering flow reorients towards the top surface and forms a strong counterclockwise recirculation zone (Figure 6b and 6d). The appearance of turbulence inhibitor provides more surface directed flow with lesser turbulence on the free surface which improves the inclusions removal efficiency and also reduce the shear stress on the walls.

In Figure 7, the predicted flow patterns show that in the bare tundish, the entering flow moves along the bottom and spreads quickly into different directions in the outlet region. In the casting chamber, a high turbulence zone is observed (Figure 7a, 7c). The existence of turbulence inhibitor impaired the turbulence zone in the outlet chamber due to the redirection of the incoming flow (Figure 7b and 7d). When the flow is controlled by the U-baffle, the incoming stream can only pass through the U-baffle through the deflector holes which located in the front and side wall of the pouring chamber. The outcoming streams form two strong recirculations nearby the holes (Figure 7c, 7d, 8c and 8d). The flow velocities in the center of the tundish increase due to the existence of the U-baffle (Figure 8c and 8d), leading to the improved mixing in the tundish.

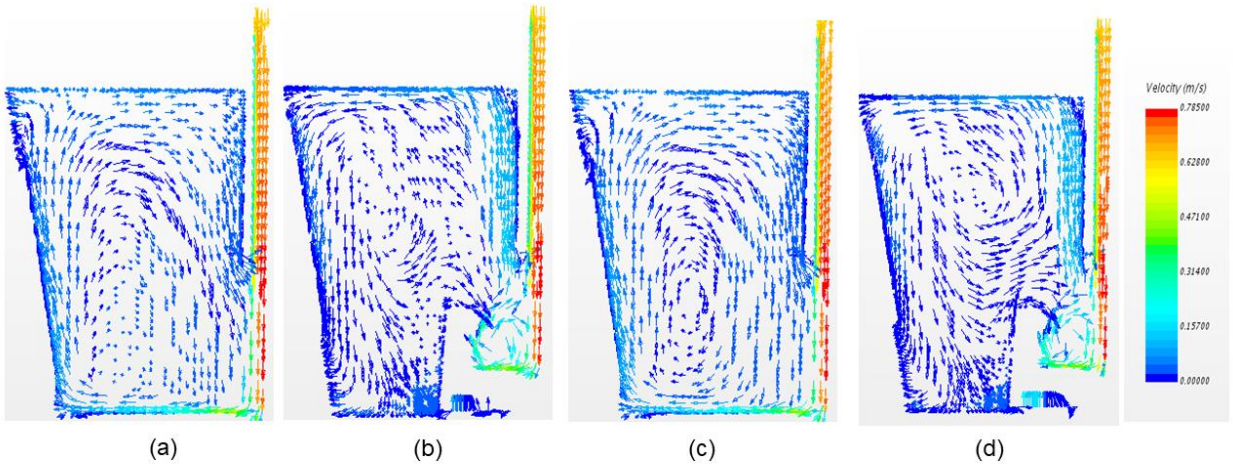

Figure 6 View A (a) Case 1-bare (b) Case 2-turbo (c) Case 3-U-baffle (d) Case 4-U-baffle+turbo

Preprints (www.preprints.org) | NOT PEER-REVIEWED | Posted: 16 July 2020 doi:10.20944/preprints202007.0354.v1

Peer-reviewed version available at Metals 2020, 10, 1084; doi:10.3390/met10081084

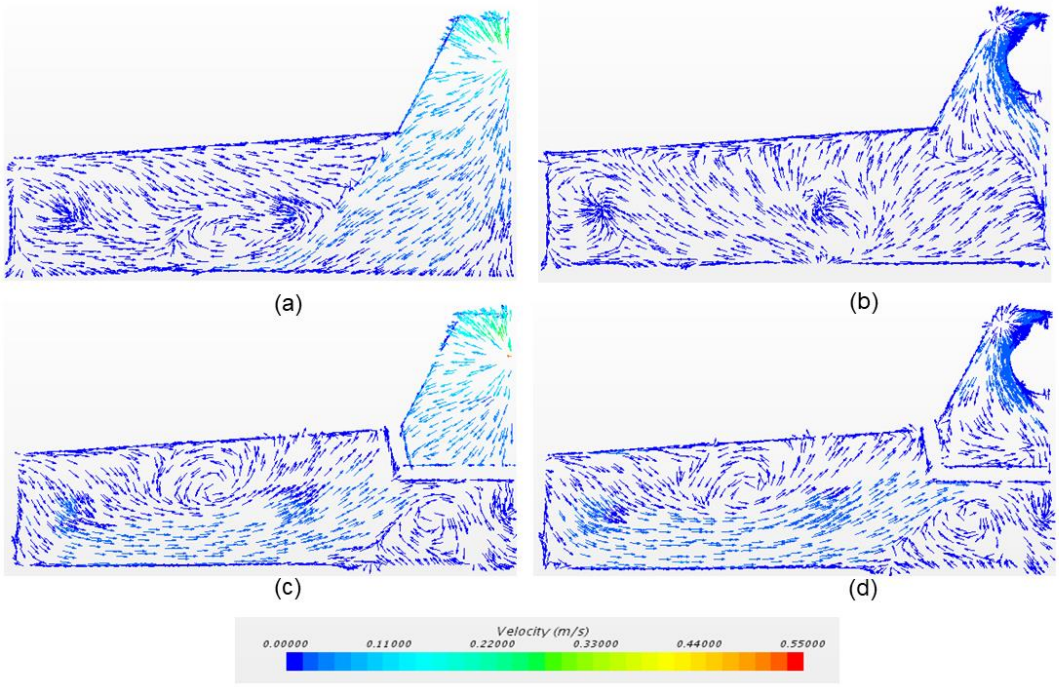

Figure 7 View B (a) Case 1-bare (b) Case 2-turbo (c) Case 3-U-baffle (d) Case 4-U-baffle+turbo

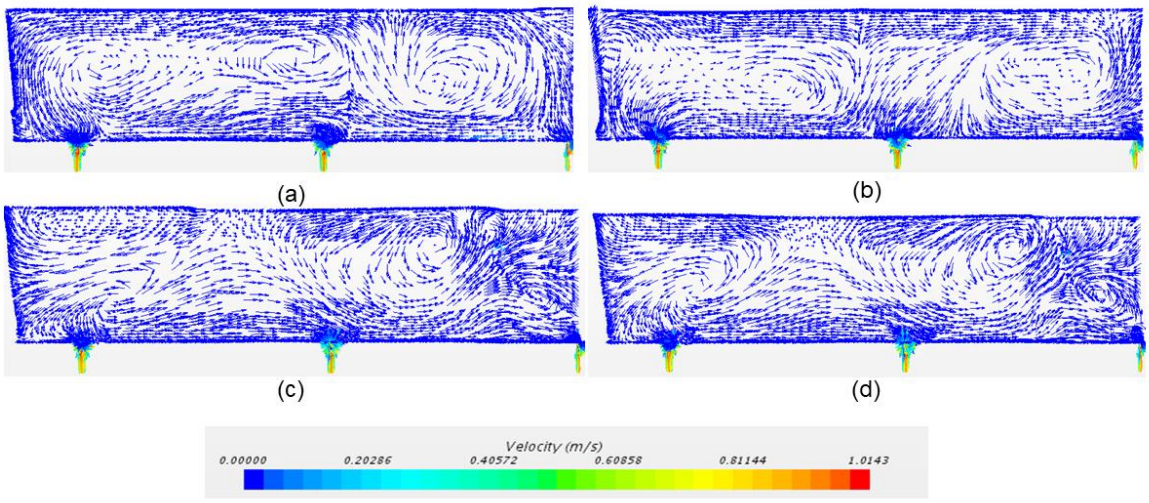

Figure 8 View C (a) Case 1-bare (b) Case 2-turbo (c) Case 3-U-baffle (d) Case 4-U-baffle+turbo

3.2 Tracer Dispersion

Figure 9 shows the comparisons between the predicted and measured results of the transient tracer dispersions for case 4-U-baffle+turbo. The tracer comes out through the deflector hole of the U-baffle, tends to flow towards to the left-side wall along the top surface. One part of the tracer flows downward towards the outlets, while another part flows straight to the left-side wall, then flows back to the outlets along the bottom of the tundish. This flow pattern extends the flow path from the inlet to the outlets, which prolongs the residence time of liquid stream and improves the mixing in the tundish.

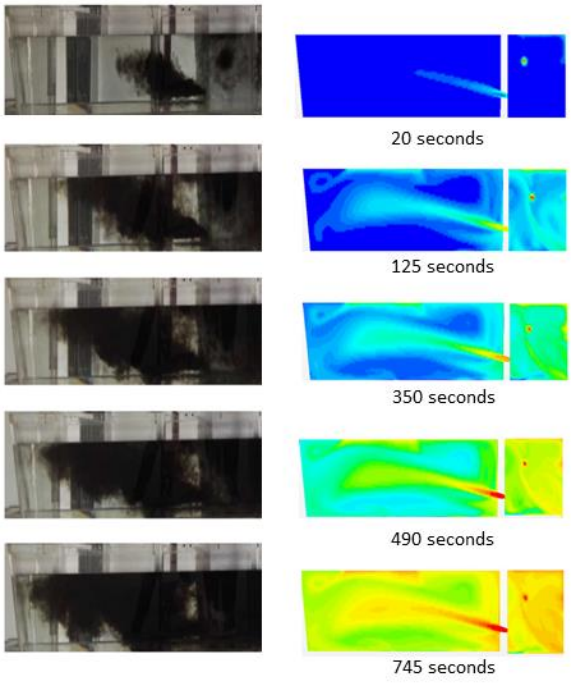

Figure 9 Tracer dispersion in case 4 (U-baffle+ turbo) in water modelling and numerical modelling

3.3 E-curve

Figure 10 gives the E-curves through the numerical simulations and experimental measurements. As shown in Figure 10a, for the outlet 1 in the bare tundish case, the calculated breakthrough and peak concentration occurs at a relatively earlier time, 4s and 36s, respectively (listed in Table 3). A sharp rising in the tracer concentration indicates a short-circuiting flow which is undesirable in the tundish. Both the experimental and numerical E-curves present double peaks at outlet 1, indicating that the bare tundish is associated with the considerable large dead volumes. The simulated dead volume fraction is up to 27%, which reduces the effective working space in the tundish.

The E-curves of the case 2-turbo are given in Figure 10b. The shape of the curves is similar as in Figure 10a. The predicated breakthrough time is 22 seconds and the dead volume fraction is 36% at outlet 1. Furthermore, the predicted mean residence time of the three outlets is 482 seconds, 673 seconds and 748 seconds, respectively, showing a significant difference.

The E-curves obtained for case 3-baffle and case 4-baffle+ turbo are analyzed in Figure 10c and 10d. The tundish equipped with the U-baffle (with deflector holes) could improve the flow characteristics by obtaining a more uniform liquid flow. The dead volume fractions are brought down less than 10% and the plug volume fractions are around 20% of the three outlets for both case 3 and case 4. The mean residence time of outlet 1 has been prolonged comparing with the cases without U-baffle. U-baffle leads to a more

Preprints (www.preprints.org) | NOT PEER-REVIEWED | Posted: 16 July 2020 doi:10.20944/preprints202007.0354.v1

Peer-reviewed version available at Metals 2020, 10, 1084; doi:10.3390/met10081084

uniform flow distribution in the tundish and minimizes the dead volume variance among the outlets. The optimal tundish should have a big volume fraction of the plug flow and a small volume fraction of the dead flow. When comparing case 3 to case 4, it shows that the turbulence inhibitor delays the breakthrough time of all the outlets but shortens the mean residence time (Table 3).

It is observed that the numerical solution differs significantly from that of the physical modelling in the initial stage, as shown in Figure 10a. The measurement uncertainties have a larger effect on the results. The possible sources of the measurement uncertainties include the mass flow rate, the amount of tracer injected, the injection rate and the conductivity measurements. As shown in Figure 10c and 10d, there is a good matching of the breakthrough time between the predicted and measured results, but the measured results show a slight right shift of the RTD curves as compared to the predicted results. The slope of E-curves after the peak is close to each other. Thus, the overall comparison between the simulation and experiment is satisfactorily close for case 3 and case 4. This is consistent with the observed dye trace dispersion (Figure 9).

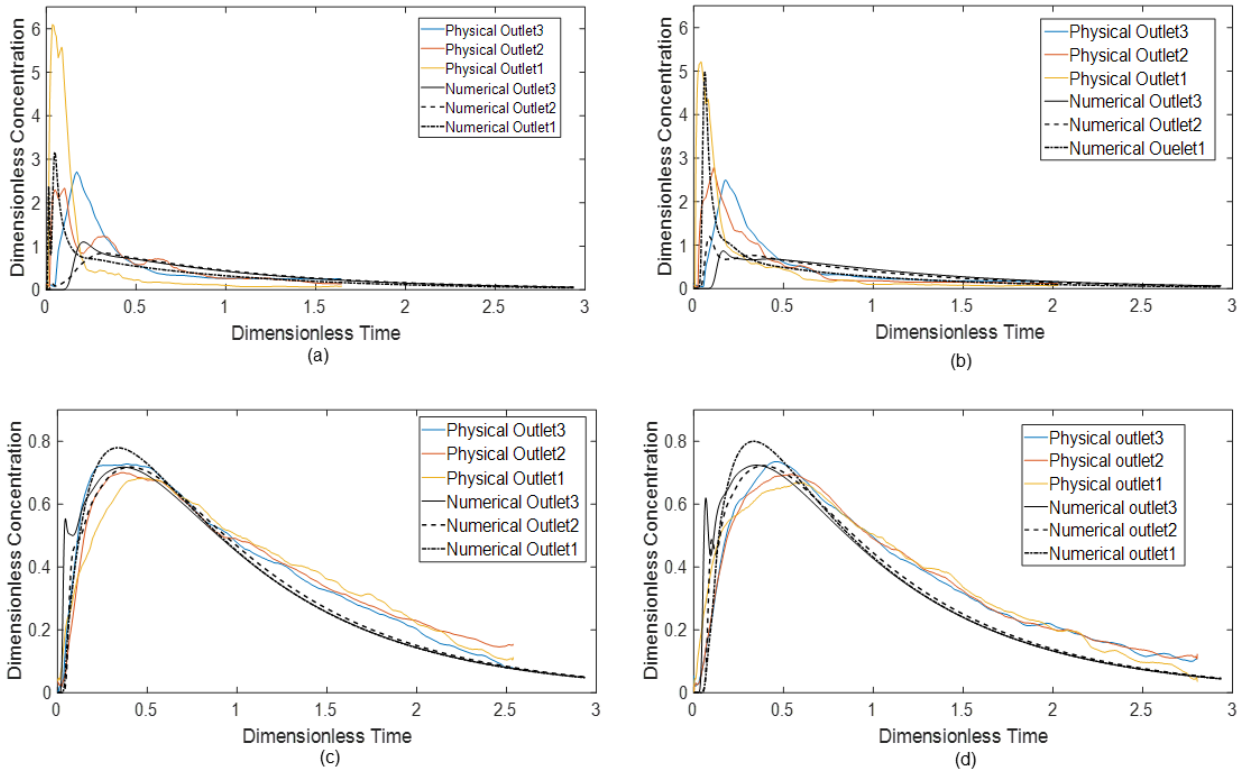

Figure 10 E-curves of the mathematical and physical model (a) Case 1-bare (b) Case 2-turbo (c) Case 3-U-baffle (d) Case 4-U-baffle+turbo (Data is available in the Supplementary Material)

Table 3 The calculated RTD parameters and the volume fraction of flow

Case	t_{theo}(s)	t_{min}(s)	t_{max}(s)	t_{mean}(s)	V_p(%)	V_m(%)	V_d(%)
1-outlet1	749	4	36	544	3	70	27
1-outlet2	749	13	239	733	17	81	2

1-outlet3	749	78	155	711	16	79	5
2-outlet1	749	22	46	482	5	60	36
2-outlet2	749	28	65	673	6	84	10
2-outlet3	749	69	123	748	13	86	1
3-outlet1	749	27	252	696	19	74	7
3-outlet2	749	32	304	716	22	73	4
3-outlet3	749	15	274	690	19	73	8
4-outlet1	749	44	250	692	20	73	8
4-outlet2	749	44	291	707	22	72	6
4-outlet3	749	27	261	682	19	72	9

3.4 F-curve

It has been a major challenge to reduce the intermixing length of continuous casting product during the ladle changeover operation. The F-curve is created by adding the tracer continuously. The F-curve results provide useful data for the prediction of the intermixing grade. Figure 11 shows the mathematical modelling results of the F-curves. The model assumes that an intermixing zone exists between the value 0.2 and 0.8 of the dimensionless concentration of the tracer.

In the case 1-bare tundish (Figure 11a), the dimensionless concentration value of 0.2 at outlet 1 requires relatively less time, about 82 seconds. This means that the new grade steel (C_{tracer}=1 at the inlet) flows along a short path to the outlet 1 as soon as it enters the tundish. The deviation for the F-curve among three outlets in case 1 and case 2 are bigger than that in case 3 and case 4. Figure 12 suggests that the predicted intermixing time related to the four studied cases. In case 4, the tundish equipped with U-baffle and turbulence inhibitor generates the shortest intermixing time and the lowest deviation among the three outlets. This means that an optimum flow control in the tundish can shorten the intermixing zones, thereby increasing the steel yields during the mixed grade continuous casting process.

Preprints (www.preprints.org) | NOT PEER-REVIEWED | Posted: 16 July 2020 doi:10.20944/preprints202007.0354.v1

Peer-reviewed version available at Metals 2020, 10, 1084; doi:10.3390/met10081084

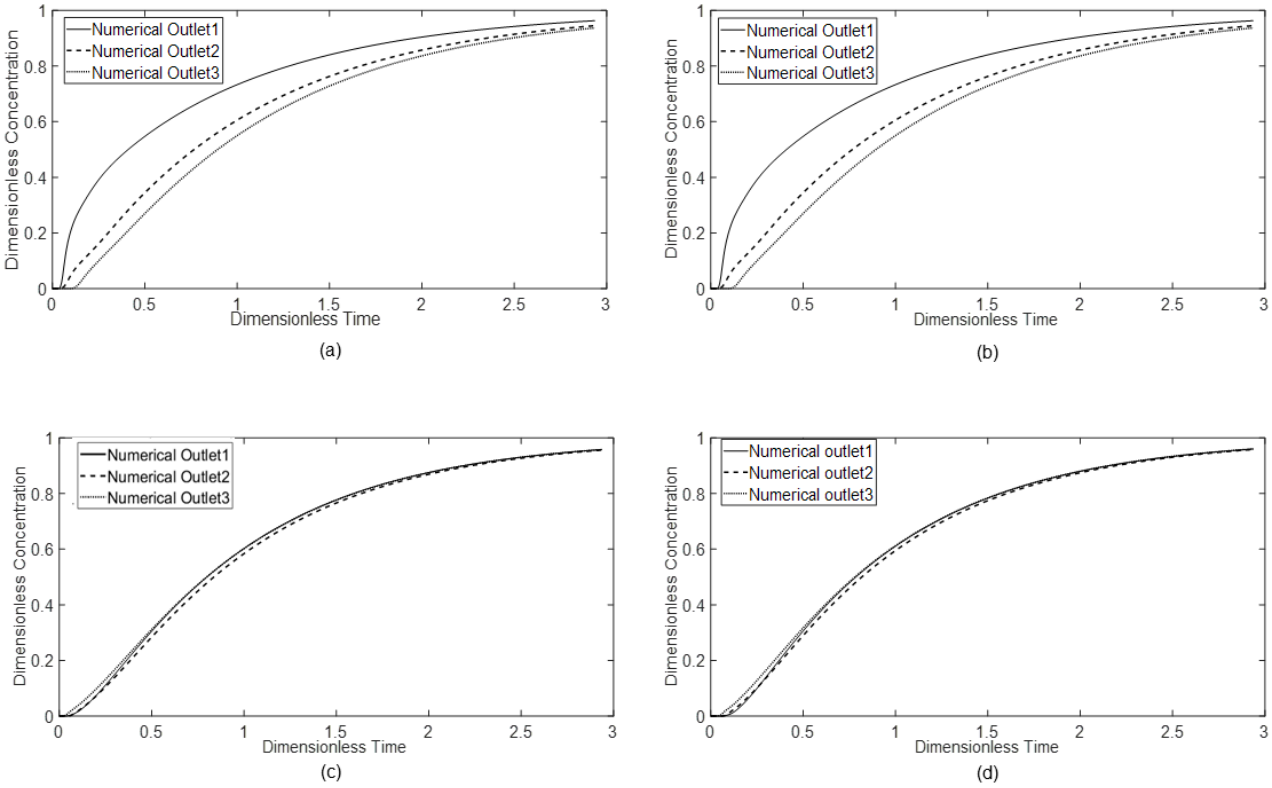

Figure 11 F-curve of the mathematical and physical model (a) Case 1-bare (b) Case 2-turbo (c) Case 3-baffle (d) Case 4-turbo+baffle (Data is available in the Supplementary Material)

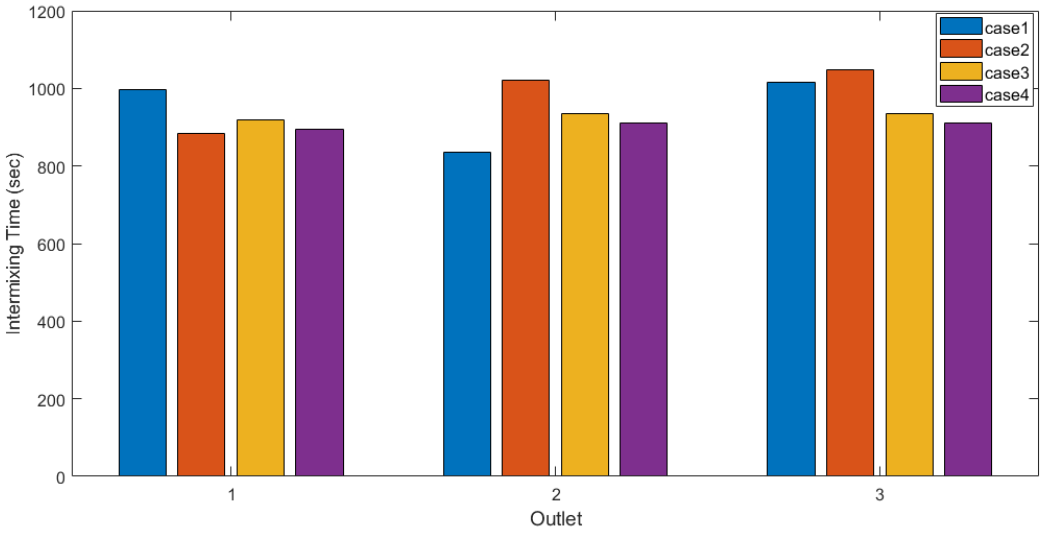

Figure 12 Predicted intermixing time during ladle changeover (Data is available in the Supplementary Material)

4 Conclusions

The fluid flow and the RTD curves associated with a five-strand tundish have been investigated through the CFD simulations and the water model experiment. Following conclusions can be drawn from the results:

- A combination of the U-baffle with deflector holes and turbulence inhibitor are proposed for a five-strand tundish. The existence of turbulence inhibitor impaired the turbulence zone in the outlet chamber due to the redirection of the incoming flow. Additionally, the U-type baffle with deflector holes can reorient the flow and extend the flow path, which is predicted by the numerical flow simulation and visualized through tracer dispersion in the water modelling.
- A sharp increase in the tracer concentration suggests the short-circuiting phenomena in the bare tundish, resulting in a relatively high dead volume fraction, up to 27%. High dead volume fraction is an undesirable feature in the tundish design.
- The tundish equipped with the U-baffle with deflector holes can improve the flow characteristics in the E-curve analysis. The dead volume fractions are less than 10% and the plug volume fractions are around 20% for all the outlets. The deviation around E-curves indicates a lowered difference of the flow characteristics among the outlets. The comparison of two U-baffle cases shows that the existence of turbulence inhibitor delays the breakthrough time but shortens the mean residence time.
- Intermixing time of the mixed grade casting are numerically investigated for the ladle changeover operation by the analysis of the F-curve. A slope change of F-curve is observed when there is a short-circuiting phenomenon. The tundish equipped with U-baffle and turbulence inhibitor generates the shortest intermixing time and the lowest deviation at the outlets.

Supplementary Material

Data for Figure 5,10,11 and 12 (Excel file)

Author Contribution

Investigation, D.Y.S.; Methodology, D.Y.S., Q.Y.; Writing—original draft preparation, D.Y.S.; Writing—review and editing, D.Y.S.; Validation, Q.Y.; Project administration and funding acquisition, D.Y.S.

Funding

This paper was supported by Swedish Foundation for Strategic Research (SSF)- Strategic Mobility Program (2019).

Acknowledgments

The work is supported by Swedish Foundation for Strategic Research (SSF) - Strategic Mobility Program (2019).

Conflicts of Interest

The authors declare no conflict of interest.

References

1 Mazumdar, D.; Guthrie, R.I.L. The Physical and Mathematical Modelling of Continuous Casting Tundish Systems. *ISIJ International* **1999**, 39, pp. 524-547.

2 Chattopadhyay, K.; Isac, M.; Guthrie, R.I.L. Physical and Mathematical Modelling of Steelmaking Tundish Operations: A Review of the Last Decade (1999–2009), *ISIJ International* **2010**, 50, pp.331–348.

3 Mazumdar, D.; Review, Analysis, and Modeling of Continuous Casting Tundish Systems, *Steel research int.* **2019**, 90, 1800279.

4 Szekely, J.; Ilegbusi, O. *The Physical and Mathematical Modeling of Tundish Operations*, Springer-Verlag ,**1989.**

5. López-Ramírez, S.; Palafox-Ramos, J.; Morales, R.D.; Barrón-Meza, M.A.; Toledo. M.V. Effects of tundish size, tundish design and casting flow rate on fluid flow phenomena of liquid steel. *Steel Research* **1998**, 69, pp. 423-428.

6. Vargas-Zamora, A.; Palafox-Ramos, J.; Morales, R.D.; Díaz-Cruz,M.; Barreto-Sandoval, J.D.J. Inertial and buoyancy driven water flows under gas bubbling and thermal stratification conditions in a tundish model. *Metallurgical and Materials Transactions B* **2004**, 35, pp. 247-257.

7. Zhong, L.C.; Li, L.Y.; Wang, B.; Zhang, L.; Zhu,L.X.; Zhang,Q.F. Fluid flow behaviour in slab continuous casting tundish with different configurations of gas bubbling curtain. *Ironmaking & Steelmaking* **2008**. 35, pp. 436-440.

8. Bensouici, M..; Bellaouar, A.; Talbi, K. Numerical Investigation of the Fluid Flow in Continuous Casting Tundish Using Analysis of RTD Curves. *Journal of Iron and Steel Research, International* **2009**, 16, pp. 22-29.

9. Zheng, M.J.; Gu, H.Z.; Ao H.; Zhang H.X.; Deng, C.J. Numerical simulation and industrial practice of inclusion removal from molten steel by gas bottomblowing in continuous casting tundish. *Journal of Mining and Metallurgy, Section B: Metallurgy*, **2011,** 47.

10. Chen, D.F.; Xie, X.; Long, M.J.; Zhang, M.; Zhang L.L.; Liao, Q. Hydraulics and Mathematics Simulation on the Weir and Gas Curtain in Tundish of Ultrathick Slab Continuous Casting. *Metallurgical and Materials Transactions B*, **2013**, 45, pp. 200.

11. Chen, C.; Jonsson L.T.I.; Tilliander, A.; Cheng G.G.; Jönsson, P.G.; A Mathematical Modeling Study of Tracer Mixing in a Continuous Casting Tundish. *Metallurgical and Materials Transactions B*, **2015**. 46, pp. 169-190.

12. Chang, S.; Zhong, L; Zou, Z. Simulation of Flow and Heat Fields in a Seven-strand Tundish with Gas Curtain for Molten Steel Continuous-Casting. *ISIJ International*, **2015**, 55, pp. 837-844.

13. Devi, S.; Singh, R.;Paul, A. Role of Tundish Argon Diffuser in Steelmaking Tundish to Improve Inclusion Flotation with CFD and Water Modelling Studies. *International Journal of Engineering Research & Technology*, **2015**. 4, pp. 213-218.

14. He, F.; Zhang, L.Y.; Xu, Q.Y.; Optimization of flow control devices for a T-type five-strand billet caster tundish: water modeling and numerical simulation. *China Foundry*, **2016**. 13, pp. 166-175.

15. Neves, L.; Tavares, R.P. Analysis of the mathematical model of the gas bubbling curtain injection on the bottom and the walls of a continuous casting tundish. *Ironmaking & Steelmaking*, **2017**. 44, pp. 559-567.

16. Wang, X.Y.; Zhao, D.T.; Qiu, S.T.; Zou, Z.S. Effect of Tunnel Filters on Flow Characteristics in an Eight-strand Tundish. *ISIJ International,* **2017,** 57, pp. 1990-1999.

17. Aguilar-Rodriguez C.E.; Ramos-Banderas, J.A.; Torres-Alonso, E.; Solorio-Diaz,G.; Hernández-Bocanegra, C.A. Flow Characterization and Inclusions Removal in a Slab Tundish Equipped with Bottom Argon Gas Feeding. *Metallurgist*, **2018**, 61, pp.1055-1066

18. Yang, B.; Lei, H.; Zhao, Y.; Xing, G.; Zhang, H. Quasi-Symmetric Transfer Behavior in an Asymmetric Two-Strand Tundish with Different Turbulence Inhibitor. *Metals*, **2019**, 9, pp. 855.

19. Wang, Q.; Liu, Y.; Huang, A.; Yan, W.; Gu, H.; Li, G. CFD Investigation of Effect of Multi-hole Ceramic Filter on Inclusion Removal in a Two-Strand Tundish. *Metallurgical and Materials Transactions B*, **2020**. 51, pp. 276-292.

20. Siemens, STAR-CCM+ version 13.04 User Guide. **2019**